



Experimental study of a broad area vertical-cavity semiconductor optical amplifier

F. Marino ^{*}, S. Balle ¹

*Dept. de Física Interdisciplinar, Instituto Mediterráneo de Estudios, Avanzados (CSIC-UIB),
C. Miquel Marqués 21, E-07190 Esporles, Spain*

Received 5 September 2003; received in revised form 26 November 2003; accepted 27 November 2003

Abstract

An experimental study of a broad-area vertical-cavity semiconductor optical amplifier in the 980 nm wavelength range is reported. We show that the gain and the saturation power in such a device increase as the transverse dimension of the injected beam is increased. A gain of 16.3 dB with 0.8 nm optical bandwidth and saturation power of 1.4 mW has been obtained. The polarization sensitivity of the device is also studied. We show that birefringence in the cavity affects the polarization insensitivity expected in ideal devices as a consequence of the circular symmetry of the cavity. A brief study of the wavelength dependence of the output transverse profile is also reported.

© 2003 Elsevier B.V. All rights reserved.

PACS: 42.65.Yj; 42.60.Da; 42.60.Jf; 42.81.Gs

Keywords: Semiconductor optical amplifiers

Semiconductor optical amplifiers (SOAs) are an interesting alternative to fiber amplifiers in optical communication systems, particularly for all the applications in which low-cost, low power consumption and compact amplifiers are required such as Fiber to the home (FTTH) applications, metro-area networks (MANs), local area network (LAN), etc. In these applications, in which the

performances of fiber amplifiers are not required, the manufacturing cost is one of the most important factors, and SOAs can fulfil most of the requirements. Although conventional SOAs have sufficient single-pass gain to operate as travelling wave amplifiers, they have poor coupling efficiency to optical fibers and are typically quite sensitive to polarization due to their planar geometry. Recently, vertical-cavity semiconductor optical amplifiers (VCSOAs) have attracted a strong research interest [1,2], because they provide a certain number of advantages respect to conventional SOAs. The vertical cavity design, in fact, allows for a better fiber coupling, on wafer testing (reducing the manufacturing costs), the possibility to

^{*} Corresponding author. Tel.: +34-971-61-17-33; fax: +34-971-61-17-61.

E-mail address: fmarino@imedea.uib.es (F. Marino).

¹ On sabbatical leave at Institut Non Linéaire de Nice (UMR 6618, UNSA-CNRS), 1361 Rte. des Lucioles, F-06560 Valbonne, France

be integrated into 2D array architectures and polarization insensitivity.

The single-pass gain in VCSOAs is smaller than in SOAs because of the shorter active region; to compensate for this, VCSOAs use feedback, provided by the cavity mirrors. Therefore, the gain spectrum of VCSOAs corresponds to the material gain spectrum convolved with the cavity resonances. Since the mirrors defining the VCSCOA cavity have usually quite high reflectivities, the gain of the VCSCOA strongly depends on the injected wavelength and an amplification is limited to wavelengths around the cavity resonances. This effect, which limits the optical bandwidth of the amplifier, can be reduced by using mirrors with lower reflectivity, but then also the amplifier gain decreases [3]. The influence of mirror reflectivity on the gain of VCSCOAs was studied in [4] by analyzing the performances of optically pumped VCSCOAs operating in the 1.3 μm wavelength region with top mirrors consisting of 12 and 13 Bragg pairs. A gain of 11.3 dB and a corresponding optical bandwidth of 0.6 nm (100 GHz) were demonstrated for the 12 top mirror period amplifier for an input signal power of -20 dBm. In the same paper also a 13 dB fiber to fiber gain is reported, but the corresponding optical bandwidth is not specified. For VCSCOAs in the 980 nm wavelength range, a maximum gain of 20 dB and an optical bandwidth of 0.1 nm were measured for an input signal of -40 dBm [5].

Another possibility for increasing the optical bandwidth of VCSCOAs is to use broad-area devices. In fact, the larger the device, the lower the frequency separation between the transverse modes and for broad-area VCSCOAs (diameter of 50 μm or more), this separation is so small that their transverse resonances form a quasi-continuous within the gain curve. Due to its transverse dimension, broad area VCSCOAs would also provide a wider gain and optical bandwidth, as well as a higher saturation power compared with smaller devices.

In this paper we study the performance of broad-area VCSCOAs in the 980 nm range. Although this is not a wavelength used in telecommunications, most of the properties that we report in this manuscript should not depend critically on

wavelength, hence they could also be of applicability whenever broad-area VCSELs at 1300 or 1550 nm become available. In particular, we report a characterization of the gain as a function of the wavelength and of the injected power for two different dimensions of the injected beam spot. We also study the polarization dependence of the gain, since VCSCOAs are expected to be polarization insensitive due to their cylindrical symmetry. Nevertheless, as we show in this paper, the VCSCOA exhibits polarization sensitivity due to the presence of residual anisotropies (birefringence and dichroism) in the cavity [6]: even though the maximum gain is almost the same for the two polarizations (which indicates a low dichroism in the cavity), the gain curves are displaced by a large amount in wavelength due to a large birefringence.

Our VCSCOA [7] is an electrically pumped, bottom-emitting, oxide-confined vertical cavity surface emitting laser whose emission wavelength is close to 980 nm. The diameter of the circular oxide window is 50 μm , and the optical cavity is defined by two Bragg mirrors consisting of 17 n-type and 30 p-type pairs. The active region consists of three quantum-wells.

The device is not lasing under continuous-wave (CW) operation. Under pulsed conditions, at room temperature, the laser threshold corresponds to a current of 300 mA. In CW conditions, the light-current curve corresponds to that of an LED reaching a maximum around 200 mA followed by thermal roll-over. The VCSCOA is biased at 180 mA and operates in reflection mode. For this current level, the amplified spontaneous emission (ASE) power is 1.5 mW, with a coupling loss of ~ 0.45 dB to the collimator. The injection beam is provided by a tunable source that consists in a 980 nm edge-emitting laser with frequency selective optical feedback through Littman external cavity and isolated from the other parts of the setup by means of an optical diode. The output (the zeroth-order reflection from the external grating) is injected into the VCSCOA (see Fig. 1). The polarization of the injected light can be changed with a half-wave plate, while the dimension of the injected beam can be controlled with a lens in front of the VCSCOA. The output of the VCSCOA is sent to a polarizer (to resolve in polarization the out-

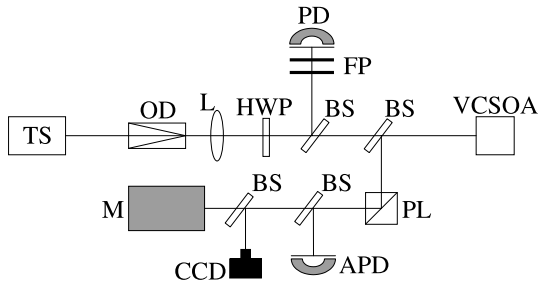


Fig. 1. The experimental setup. TS: tunable source, OD: optical diode, HWP: half-wave plate, L: lens, BS: beam-splitter, FP: Fabry–Perot interferometer, PD: photodiode, PL: linear polarizer, CCD: CCD camera, M: monochromator.

put) and then to the monochromator (optical bandpass of 0.05 nm) which allows us to evaluate the amplifier gain without the contribution of the spontaneous emission noise.

In the first measurement, the injected beam is focalised on the VCISOA mirror, such that its diameter is $\approx 10 \mu\text{m}$. We fix the position of the half-wave plate in order to inject horizontal polarization and we measure the gain dependence on the wavelength and the power of the injected signal. Fig. 2 (open symbols) shows the gain versus wavelength for an input power of 0.1 mW, while in the inset is reported the gain maximum versus injected power. We obtain a maximum gain of 12.5

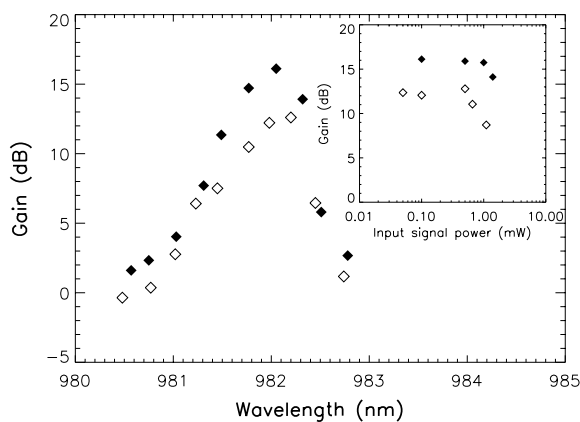


Fig. 2. Gain versus wavelength for an input power level of -10 dBm focused to a diameter of $10 \mu\text{m}$ (open symbols) and $50 \mu\text{m}$ (solid symbols). In the inset, we plot the maximum of the gain spectrum for different input powers for the two cases (symbols as above).

dB and an optical bandwidth of 215 GHz (0.7 nm). The VCISOA gain remains constant within our measurement error (≈ 0.5 dB) until the injected optical power approaches 1 mW. The saturation injected power, corresponding to a 3 dB drop in the gain, is at ≈ 0.7 mW. The solid symbols in Fig. 2 correspond to a beam whose diameter is almost the same than that of the VCISOA ($\approx 50 \mu\text{m}$). In this case, we obtain a higher saturation optical power (3 dB drop at ≈ 1.4 mW) and a higher gain (16.3 dB) than for the smaller beam. Also the optical bandwidth is larger (0.8 nm, i. e. 245 GHz), although its enhancement is smaller than those observed in the gain and in the saturation power. In our opinion, the gain enhancement for the larger beam is due to the larger active medium surface now involved in the amplification process, together with the consequent lower injected power density. Although it cannot be excluded that some degree of current crowding at the edges of the aperture contributes to the higher gain, in our device we have quite a uniform distribution of ASE at 180 mA, with a total variation of less than 5% between the edges of the oxide window and the center.

It is worth noting that when scanning the wavelength of the injected field, the profile of the VCISOA output changes. In fact, the output beam profile will remain essentially constant only in small devices (diameter $< 5 \mu\text{m}$) with a structure that supports just the fundamental transverse mode, but in this case the optical bandwidth is limited to the linewidth of the Fabry–Perot mode. In larger devices that support many higher order transverse modes, the output profile will in general depend on the injected wavelength. In broad area devices, the wavelength dependence of the reflected beam profile can be enhanced because dispersion and gain or absorption may dominate over the transverse boundary conditions. In these conditions, a homogeneous injected beam can yield a non-homogeneous output due to a modulational instability originating from stimulated emission inside the cavity [8]. This is a nonlinear process, since changes in the carrier density are accompanied by a shift of the cavity resonance through changes in the carrier-induced refractive index, which in turn implies a change in the intracavity field producing stimulated emission. Several

spatial structures like ring and hexagonal patterns [8], beam filamentation [9] and even the formation of localized structures [10] can be found depending on the system parameters.

In Fig. 3 we show, for the same parameters as in Fig. 2, the evolution of the output profile as the wavelength of the injected field is tuned. For short wavelengths (input field to the blue of the maximum in the gain curve) the transverse profile consists of slightly-modulated ring patterns whose characteristic wave vector diminishes almost linearly as the detuning decreases [11]. Approaching the gain maximum, the rings start to break, the length scale of the pattern becomes of the order of the VC SOA aperture and finally a single, bright spot remains (see middle right and lower left panels in Fig. 3). It is worth noting that these patterns are not simple superpositions of Gauss–Laguerre or Gauss–Hermite patterns [11], but that they appear because of the previously mentioned modulational instability due to the large diameter of our device,

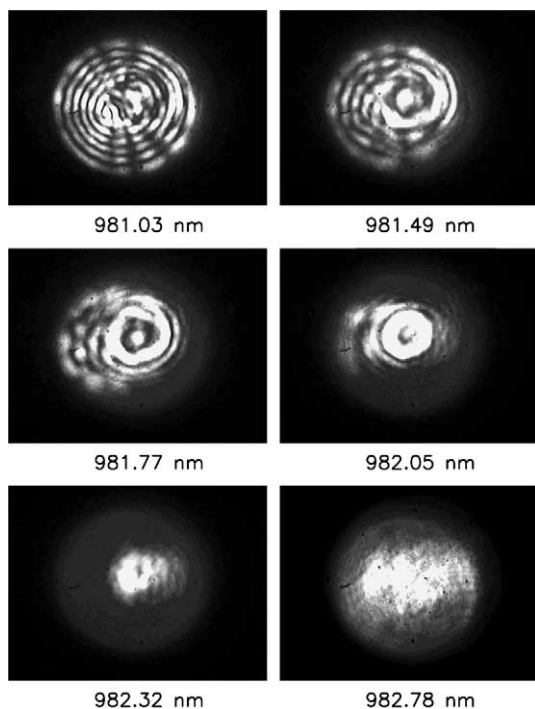


Fig. 3. Near-field images for a $\approx 50 \mu\text{m}$ diameter injected beam. The pumping current is 180 mA and the injected power is $\approx 0.8 \text{ mW}$.

as evidenced by their dependence on the injected power [12]; indeed, for very low injected powers only the diffraction rings are observed. As the injection wavelength is further increased, the intracavity field is strongly reduced, the modulational instability that led to the formation of the patterns disappears, and the profile of the reflected beam is essentially that of the injected beam.

A similar sequence can also be observed by fixing the wavelength and changing the current injected into the VC SOA, which can be understood as the thermal tuning of the cavity resonance due to Joule heating of the VC SOA. The length scale of the pattern does not significantly depend on the diameter of the injected beam, although for smaller spots a wider range of transverse wave-vectors is observed.

The large diameter of our device enables us to obtain much larger gain bandwidths than previously reported at the price of a non-constant output profile. In practical applications this changing field profile will reduce the fiber-coupling efficiency. If the coupling losses are too large – or in applications like wavelength conversion whose efficiency is always rather small – in-line amplification of the signal can be performed in order to attain acceptable power levels.

We next determine the polarization sensitivity of the VC SOA. We set the input beam power to 0.1 mW and the beam diameter to $\approx 50 \mu\text{m}$, and we measure the gain spectrum of the device for horizontal and vertical polarizations of the input beam. The results are shown in Fig. 4, and it can be observed that although the peak gain and optical bandwidth are almost the same for both polarization orientations, the corresponding gain spectra are shifted by $\approx 0.2 \text{ nm}$. We have checked that this relative displacement of the two gain spectra does not depend on the input power, and in all cases we obtain approximately the same maximum gain and optical bandwidth for both polarizations (see inset in Fig. 4). The same measurements for the smaller beam diameter lead to the same shift of the polarization-resolved gain spectra. The precision of our measurement does not allow for determining the gain differences that might exist due to dichroism in the VC SOA cavity and which are at most of 0.3 dB.

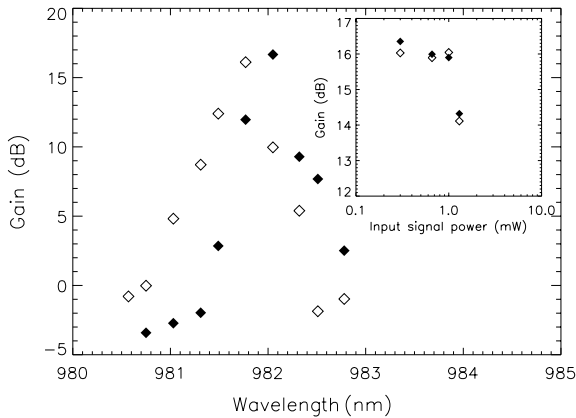


Fig. 4. Gain versus wavelength for vertical (open symbols) and horizontal (solid symbols) polarizations of the input signal when the beam diameter is 50 μm and the input power 0.1 mW. Inset: maximum gain versus input signal power for the same conditions (symbols as above).

Such a kind of polarization sensitivity can be attributed to birefringence in the cavity, which breaks its cylindrical symmetry and lifts the frequency degeneracy between orthogonally polarized transverse modes. In fact, the polarization resolved ASE curves of the VC SOA (see Fig. 5) exhibit the same features as the VC SOA gain spectra, with a separation between the two maxima of 0.17 nm, corresponding to ≈ 50 GHz. The typical values for birefringence reported in litera-

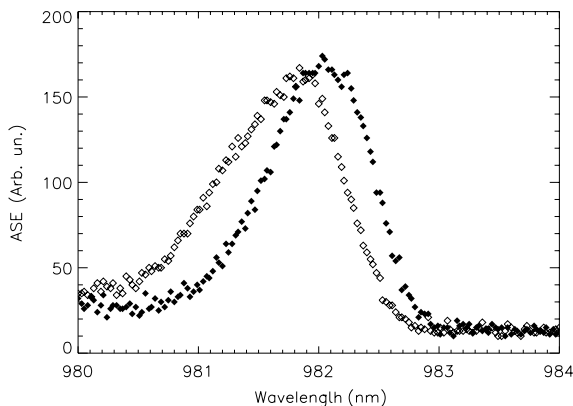


Fig. 5. Polarization resolved ASE spectra at the working current (180 mA). Open symbols correspond to vertical polarization and solid symbols to the horizontal one.

ture range from 5 to 25 GHz [13,14], but also birefringence values as high as 50 GHz have been measured in oxide-confined VCSELs [15]. As reported in [14], these residual anisotropies can have their origin in the electro-optic and elasto-optic effects. The first is due to the electrical pumping of the device together with the built-in fields at heterojunctions due to the different doping levels. The second is less controllable and predictable, and it arises due to the presence of residual and unintentional strain in the structure induced either during growth or due to the mounting and packaging processes. It is worth noting that the ASE power in the horizontal polarization is slightly higher than that in the vertical direction by $\approx 7\%$, which agrees with the maximum gain difference between both polarizations that was found before. This indicates that dichroism is probably not negligible in this device, as it has been already noticed in studies of the polarization dynamics of VCSELs [6,16]. As evidenced by these earlier studies, dichroism may depend quite strongly on stress induced during the mounting and packaging of the device, thus leading to important variations from one device to the other. Thus, in order to achieve truly polarization independent gain behaviour for VC SOAs, careful mounting of the devices is needed to avoid stress-induced birefringence and dichroism.

In conclusion, we have experimentally characterized the properties of a 50 μm active diameter VC SOAs, operating in the 980 nm wavelength range. We have presented results for two transverse dimension of the injected beam. When the diameter of the injected beam is comparable to the transverse diameter of the VC SOA (50 μm) a gain of 16.3 dB with 0.8 nm optical bandwidth and saturation input power of 1.4 mW have been demonstrated. For beams of smaller diameters, the peak gain and saturation input power are reduced, but the optical bandwidth is only slightly affected. These results confirm that broad-area VC SOAs can offer substantial gain and optical bandwidth. We have also found that, although the gain peak and optical bandwidth in both polarizations are the same, the VC SOA is polarization sensitive due to the birefringence of the cavity, which shifts the gain spectra.

Acknowledgements

We acknowledge financial support from MCYT (Spain) through project TIC2002-04255 and from the EU through project VISTA, HPRN-CT-2000-00034. SB acknowledges financial support from MEC (Spain) through the sabbatical grant PR2002-0329. We thank ULM University for providing us the VCSEL in the framework of the project VISTA.

References

- [1] S. Bjorlin, J. Piprek, B. Riou, A. Keating, P. Abraham, Y.C. Chiu, J.E. Bowers, 1.3-micron vertical cavity amplifier, in: Presented at the 25th Optical Fiber Communications Conference, Baltimore, MD, 2000.
- [2] D. Wiedenmann, B. Moeller, R. Michalzik, K.J. Ebeling, *Electron. Lett.* 32 (1996) 342.
- [3] C. Tombling, T. Saito, T. Mukai, *IEEE J. Quantum Electron.* 30 (1994) 2491.
- [4] E.S. Bjorlin, B. Riou, P. Abraham, J. Piprek, Y.J. Chiu, K.A. Black, A. Keating, J. Bowers, *IEEE J. Quantum Electron.* 37 (2001) 274.
- [5] D. Wiedenmann, C. Jung, M. Grabherr, R. Jager, U. Martin, R. Michalzik, K.J. Ebeling Oxide-Confined vertical-cavity semiconductor optical amplifier for 980 nm wavelength CLEO 98 Tech. Dig. 1998 Paper CThM5, p. 378.
- [6] A.K. Jansen van Doorn, M.P. van Exter, J.P. Woerdman, *Electron. Lett.* 30 (1994) 1941.
- [7] M. Miller et al., *IEEE J. Select. Topics Quantum Electron.* 7 (2001) 210.
- [8] M. Brambilla, L. Lugiato, F. Prati, L. Spinelli, W. Firth, *Phys. Rev. Lett.* 79 (1997) 2042.
- [9] Z. Dai, Annual Report 1995, Dept. of Optoelectronics, University of Ulm, Germany.
- [10] S. Barland et al., *Nature* 419 (2002) 699.
- [11] T. Ackemann et al., *Optics Lett.* 25 (2000) 814.
- [12] S. Barland et al., *Appl. Phys. Lett.* 83 (2003) 2303.
- [13] T. Ackermann, M. Sondermann, *Appl. Phys. Lett.* 78 (2001) 3574.
- [14] P. Debernardi, G.P. Bava, C. Degen, I. Fischer, W. Elsasser, *IEEE J. Quantum Electron.* 38 (2002) 73.
- [15] J.P. Hermier, A. Bramati, A.Z. Khoury, V. Josse, E. Giacobino, P. Schnitzer, R. Michalzik, K.J. Ebeling, *IEEE J. Quantum Electron.* 37 (2002) 87.
- [16] B. Ryvkin et al., *J. Opt. Soc. Am. B* 16 (1999) 2106; M.P.v. Exter, M.B. Willemsen, J.P. Woerdman, *Appl. Phys. Lett.* 74 (1999) 2274.